Journal of Drug Targeting, 2010, 1–16, Early Online

ORIGINAL PAPER

Bisphosphonate-coated BSA nanoparticles lack bone targeting after systemic administration

Guilin Wang[1], Cezary Kucharski[1], Xiaoyue Lin[1], and Hasan Uludağ[1,2,3]

[1]*Department of Chemical & Materials Engineering, Faculty of Engineering, University of Alberta, Edmonton, Alberta, Canada T6G 2G6,* [2]*Faculty of Pharmacy and Pharmaceutical Sciences, University of Alberta, Edmonton, Alberta, Canada T6G 2G6, and* [3]*Department of Biomedical Engineering, Faculty of Medicine & Dentistry, University of Alberta, Edmonton, Alberta, Canada T6G 2G6*

Abstract

A polymeric conjugate of polyethyleneimine-graft-poly(ethylene glycol) and 2-(3-mercaptopropylsulfanyl)-ethyl-1,1-bisphosphonic acid (PEI-PEG-thiolBP) was prepared and used for surface coating of bovine serum albumin (BSA) nanoparticles (NPs) designed for bone-specific delivery of bone morphogenetic protein-2 (BMP-2). The NP coating was achieved with a dialysis and an evaporation method, and the obtained NPs were characterized by particle size, ζ-potential, morphology, and cytotoxicity *in vitro*. The particle size and surface charge of the NPs could be effectively tuned by the PEG and thiolBP substitution ratios of the conjugate, the coating method, and the polymer concentration used for coating. The PEG modification on PEI reduced the toxicity of PEI and the coated NPs, based on *in vitro* assessment with human C2C12 cells and rat bone marrow stromal cells. On the basis of an alkaline phosphatase (ALP) induction assay, the NP-encapsulated BMP-2 displayed full retention of its bioactivity, except for BMP-2 in PEI-coated NPs. By encapsulating ^{125}I-labeled BMP-2, the polymer-coated NPs were assessed for hydroxyapatite (HA) affinity; all NP-encapsulated BMP-2 showed significant affinity to HA as compared with free BMP-2 *in vitro*, and the PEI-PEG-thiolBP coated NPs improved the *in vivo* retention of BMP-2 compared with uncoated NPs. However, the biodistribution of NPs after intravenous injection in a rat model indicated no beneficial effects of thiolBP-coated NPs for bone targeting. Our results suggested that the BP-conjugated NPs are useful for localized delivery of BMP-2 in bone repair and regeneration, but they are not effective for bone targeting after intravenous administration.

Keywords: *Albumin nanoparticles; bisphosphonate; bone morphogenetic protein-2; bone targeting; drug delivery*

Introduction

Nanoparticulate colloid systems have been employed in drug delivery and targeting systems, since they have the potential of selective targeting of drugs to specific tissues and cells (Schäfer et al., 1992; Wang et al., 2005; Owens & Peppas, 2006). Albumin is an endogenous protein suitable for the preparation of particulate drug delivery systems due to its natural biodegradability, biocompatibility, and non-toxicity in physiological systems (Merodio et al., 2001; Segura et al., 2005; Dreis et al., 2007). Size and surface characteristics of nanoparticles (NPs), including surface charge and hydrophilicity, can significantly influence the distribution of administered formulations in the body (Owens & Peppas, 2006). The surface properties of albumin NPs may be mediated through adsorption or conjugation with other compounds, such as targeting ligands with antibodies and poly(ethylene glycol) (PEG) polymers. PEG is an amphiphilic polyether diol, which is non-toxic and has been approved by FDA for human intravenous, oral, and dermal application. PEG has also been widely used to improve the solubility (Bronich et al., 1998) and biocompatibility of macromolecules (Tang et al., 2003; Sung et al., 2003), to prevent particulate aggregation, and to reduce their interaction with blood components (Ogris et al., 1999). A large volume of

Address for Correspondence: Hasan Uludağ, #830, Chemical and Materials Engineering Building, University of Alberta, Edmonton, Alberta, Canada T6G 2G6. E-mail: hasan.uludag@ualberta.ca

(Received 27 November 2009; revised 07 January 2010; accepted 13 January 2010)

ISSN 1061-186X print/ISSN 1029-2330 online © 2010 Informa UK Ltd
DOI: 10.3109/10611861003622560

research has shown that PEG modification on biomolecules can effectively reduce reticuloendothelial system (RES) clearance and prolong blood circulation time of the biomolecules (Soppimath et al., 2001; Harris & Chess, 2003; Owens & Peppas, 2006). PEGylated human serum albumin (HSA) NPs were studied by Mishra et al. (2006) for brain targeting delivery of an antiviral drug, azidothymidine, and enhancement of brain localization of azidothymidine was observed for transferrin anchored PEGylated albumin NPs. Lin et al. (1994, 1997, 1999) reported preparation of HSA NPs sterically stabilized with PEGylated copolymers. The existence of a hydrated steric barrier surrounding the NPs was verified and the surface-modified particles were shown to reduce plasma protein adsorption compared with unmodified surfaces.

For the development of a bone-targeting drug delivery system, another critical requirement is imparting the NPs with strong bone affinity. Bisphosphonates (BPs) have been proven to be a class of molecules with exceptional affinity to bone mineral hydroxyapatite (HA), and have been used as bone-targeting agents for several classes of drugs (Wang et al., 2005). Successful targeting of BP conjugates were obtained with several proteins, including lysozyme, BSA, and IgG (Uludag & Yang, 2002; Bansal, Gittens, & Uludag, 2004; Bansal et al., 2005). Upon systemic injection, significantly increased bone deposition (as much as sevenfold) of the BP conjugated proteins was observed. However, the direct coupling of BPs to proteins might be problematic for sensitive proteins, since the covalent conjugation of BPs to proteins may result in loss of their native bioactivity. As an alternative, BPs can be conjugated to polymeric materials, such as polylactic-co-glycolic acid (PLGA) (Choi & Kim, 2007), poly[*N*-(2-hydroxypropyl)methacrylamide] (PHPMA) (Wang et al., 2003), polyethyleneimine (PEI), and poly-L-lysine (PLL) (Zhang et al., 2007), which might be a preferable platform for delivering sensitive therapeutic agents to bone once the therapeutic agents are appropriately formulated with such polymers.

We recently optimized a coacervation procedure for the preparation of BSA NPs (Wang et al., 2008), and proposed PEI-stabilized BSA NPs for the delivery of growth factors [e.g., bone morphogenetic protein-2 (BMP-2)]. This system was shown to reasonably control the release rate of encapsulated proteins with full retention of the bioactivity of the released protein (Zhang et al., 2008). However, the toxicity of PEI and its undesirable capacity to aggregate particles were two concerns when it was used to coat the albumin NP surfaces. PEG modification of PEI might be advantageous in this respect. PEG-modified PEI has been studied for improved gene delivery (Ogris et al., 1999; Tang et al., 2003; Sung et al., 2003), and showed that PEG modification of PEI reduced its toxicity and increased their solubility. In addition, PEG with dual functional groups at its terminal ends offer the possibility of further conjugating bioactive agents or targeting moieties to PEI.

In the present study, PEI was substituted with PEG (PEI-PEG), which was then conjugated with a thiolBP (2-(3-mercaptopropylsulfanyl)-ethyl-1,1-bisphosphonic acid; PEI-PEG-thiolBP) for bone targeting. The PEI-PEG and PEI-PEG-thiolBP were used for NP coating via simple electrostatic interaction between the negatively charged BSA surfaces and the cationic PEI backbone. The PEG chains were expected to coat and stabilize the BSA/PEI core, and present thiolBP ligands on the surface. The physicochemical and biological properties, including particle size, surface charge, cytotoxicity, and BMP-2 activity, were characterized *in vitro*, as well as bone mineral affinity in an implant and an intravenous injection model in rats.

Materials and methods

Materials

ThiolBP was synthesized as described previously (Bansal et al., 2005). Branched PEI (MW ~25 kDa), BSA, ascorbic acid, 3-(4,5-dimethylthiazol-2-yl)-2,5-diphenyl-tetrazolium bromide (MTT), *p*-nitrophenol phosphate (*p*-NPP), and picrylsulfonic acid solution (TNBS; 5% w/v) were obtained from Sigma-Aldrich (St. Louis, MO, USA). The heterobifunctional PEG derivative, maleimide PEG *N*-succinimide ester (NHS-PEG-MAL; MW 3500 Da) was obtained from JenKem Technology (Allen, TX, USA). Recombinant human bone morphogenetic protein-2 (BMP-2) was expressed in *Escherichia coli* and purified as described previously (Nickel et al., 2001). $Na^{125}I$ (in 0.1 M NaOH) was purchased from GE Healthcare (Piscataway, NJ, USA). Synthetic HA was prepared according to the method described in Zhang et al. (2007). Sterile saline (0.9% NaCl, non-pyrogenic) used for implantation and injection was obtained from Baxter Corporation (Toronto, ON, Canada). The Spectra/Por dialysis tubing with molecular weight cut-off (MWCO) of 12–14 kDa was acquired from Spectrum Laboratories (Rancho Dominguez, CA, USA) and used in all dialysis procedures. Dulbecco's modified Eagle's medium (DMEM), Hank's balanced salt solution (HBSS), GlutaMax-1, penicillin (10,000 U/mL), and streptomycin (10,000 μg/mL) were from Invitrogen (Carlsbad, CA, USA). Fetal bovine serum (FBS) was from Atlanta Biologics (Atlanta, GA, USA). All tissue culture plasticware were from Corning (Corning, NY, USA). Distilled/de-ionized water (ddH_2O) used for buffer preparation and dialysis was derived from a Milli-Q purification system (Millipore, Billerica, MA, USA). Skelite™ implants, a multiphase calcium phosphate matrix (67% Si-stabilized tricalcium phosphate and 33% HA), were obtained from Millenium Biologix Inc. (Mississauga, Ontario, Canada).

Synthesis of PEI-PEG-thiolBP

The thiolBP was conjugated to branched PEI by using heterobifunctional PEG derivative (NHS-PEG-MAL) as shown in Scheme 1. The NHS-PEG-MAL and thiolBP were separately dissolved in 0.1 M phosphate buffer (pH 7.2), and mixed at equal volumes under constant shaking at 400 rpm for 1 h to obtain the NHS-PEG-thiolBP. Various volumes of NHS-PEG-thiolBP were then added to a PEI solution at 2 mg/mL (the feed ratios shown in Figure 2) in 0.1 M phosphate buffer (pH 7.2), and incubated for 3 h at room temperature while stirring. For comparison, PEI-PEG was synthesized by reacting NHS-PEG-MAL with PEI (both in 0.1 M phosphate buffer) with different molar ratios. The final products, PEI-PEG-thiolBP or PEI-PEG, were purified by dialyzing against excess 0.1 m carbonate buffer (pH 10.0, ×3) and against distilled/de-ionized water (ddH_2O, ×2).

Analysis of PEI-PEG-thiolBP

The PEG graft ratio on the PEI backbone was determined from ^{1}H-NMR spectra (analyzed after dissolving the polymer in D_2O). The BP conjugation efficiency (i.e., the average number of thiolBP per PEI) was calculated by dividing the thiolBP concentration by the PEI concentration in the samples. PEI concentrations were determined by a copper/PEI complex assay (Perrine & Landis, 1967; von Harpe et al., 2000). For this, 100 µL of samples was added to 100 µL of 20 mM $CuSO_4$ solution, and the mixture was diluted to 500 µL with 0.1 M acetate buffer (pH 5.4). Known concentrations of native PEI served as the calibration standards, and the absorbance was read at 630 nm by a UV spectrophotometer (Ultrospec@2000; Pharmacia Biotech). A phosphate assay described by Ames (1966) was used to determine the thiolBP content in the samples. An aliquot of 50 µL of sample was mixed with 30 µL of 10% $Mg(NO_3)_2$ in 95% ethanol in glass tubes and ashed over a flame. After boiling in 300 µL of 0.5 N HCl for 15 min, 600 µL of $(NH_4)_6Mo_7O_{24}$ (0.42% w/v in 1 N H_2SO_4) and 100 µL of ascorbic acid (10% w/v) were added to the tubes and the samples were incubated at 37°C for 1 h. The absorbance was determined at 820 nm, and a calibration curve based on known concentrations of thiolBP was used to calculate the concentrations of conjugated BP.

In vitro *HA affinity of polymers*

The mineral affinity of the polymers was investigated by using a HA binding assay. An aliquot of 100 µL of polymer sample was diluted to 500 µL with phosphate buffer (pH 7.0) to give 0.1 m phosphate concentration. The diluted samples were then added to 1.5 mL microcentrifuge tubes

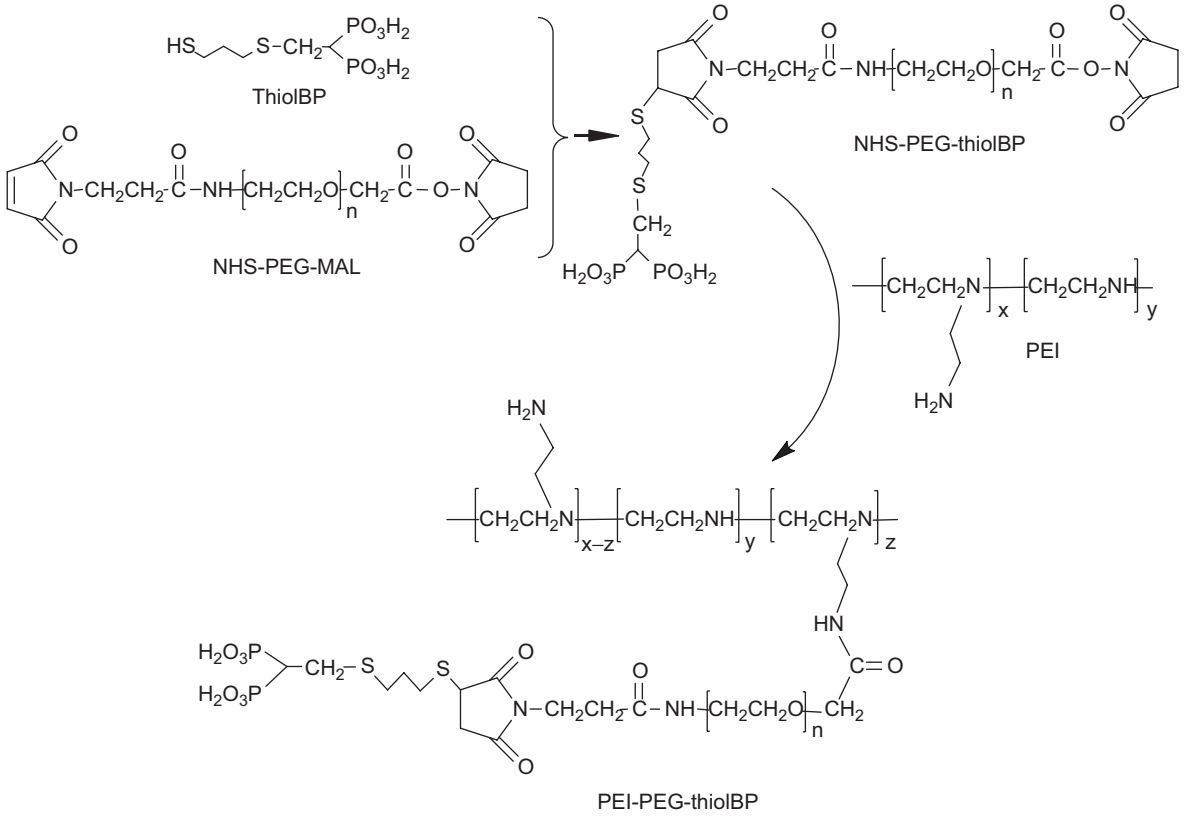

Scheme 1. ThiolBP conjugation to PEI via NHS-PEG-MAL.

containing 5 mg of HA in duplicate. As a control (i.e., 0% of binding), the samples were incubated in tubes without HA. The tubes were incubated at room temperature on an orbital shaker for 3 h, and centrifuged to separate the supernatant from the HA. A TNBS assay (Bullock et al., 1997) was used for the assessment of polymer concentrations in solution (based on amine groups). For this, 20 μL of the supernatant or control samples, or 20 μL of water as background, 130 μL of 0.1 M phosphate buffer (pH 7.0) and 850 μL of 1 mM TNBS in borate buffer (pH 9.4) were added to a cuvette, and the samples were incubated for 1 h at 37°C. The absorbance of the solutions was read at 367 nm. The percentage of bound polymer to HA (% HA binding) was calculated by using the absorbance in supernatant and control as: 100% × (Absorbance of control – Absorbance of supernatant)/(Absorbance of control – Absorbance of background).

Preparation of polymer-coated NPs

The BSA NPs were prepared by a coacervation method as described in our previous study (Wang et al., 2008). Briefly, 10 mg/mL BSA solution was first mixed with equal volume of 10 mM phosphate buffer (pH 7.4) for 15 min under constant stirring at 600 rpm. Then, acetone was added dropwise to the BSA solution as a desolvating agent until an acetone:water volume ratio of 4:1 was reached, followed by further stirring over 2 h. The resulting BSA NP suspension was retained in the acetone/water system for polymer coating.

Two methods were utilized for the preparation of polymer-coated NPs, namely a dialysis and an evaporation method. In the dialysis method, an appropriate amount of PEI, PEI-PEG, or PEI-PEG-thiolBP was dissolved in 10 mM phosphate buffer solution (pH 7.4). An aliquot of BSA NP suspension was mixed with the same volume of polymer solution at various concentrations (1–12 μM; see figure legends for exact values). The final polymer concentrations in the NP suspension were 0.5–6 μM. As a control, the uncoated BSA NPs were incubated with 10 mM phosphate at the same dilutions. The mixture was incubated at room temperature for 1 h, and then dialyzed against 1 mM NaCl (×3) to remove the acetone. For the evaporation method, an aliquot of BSA NP suspension was mixed with PEI-PEG or PEI-PEG-thiolBP as described earlier, the polymer was dispersed in a mixture of acetone/water (4:1) and the acetone was evaporated in a flowhood by constant stirring overnight.

Characterization of polymer-coated NPs

The zeta (ζ) potential of the NPs was investigated by laser Doppler anemometry using the Malvern Zetasizer 3000HS (Malvern Instruments Ltd, UK) at 25°C. Before the analysis, the polymer-coated NPs were diluted to a BSA concentration of 0.1 mg/mL with 1 mM NaCl. An electric field of 150 mV was applied to observe the electrophoretic velocity of the particles. The particle sizes and size distributions of the NPs were measured by photon correlation spectroscopy (PCS) using the same instrument. The measurements were carried out at 25°C using a 633 nm He–Ne laser at a scattering angle of 90°. The reported sizes and ζ-potentials were derived from three independent batches of NP preparations.

Atomic force microscopy (AFM) was used to observe the size and morphology of the PEI-PEG-thiolBP coated BSA NPs (MFP-3D; Asylum Research, Santa Barbara, CA, USA). The NP sample was appropriately diluted to visualize individual particles and 5 μL of the diluted sample was dropped onto the surface of PELCO Mica Discs (TED PELLA, Inc., Redding, CA, USA), and observed in a tapping mode by AC240TS cantilever after drying under room temperature. Images were processed and analyzed by the Igor Pro imaging software (version 5.04B).

Cytotoxicity of polymers and NPs by MTT assay

Two types of cells, human C2C12 myoblast cells and primary rat bone marrow stromal cells (BMSCs), were used for the assessment of the cytotoxicity of the polymers and polymer-coated BSA NPs. Both cells were cultured in an osteogenic medium, where the basal medium (high-glucose DMEM, 10% FBS, 100 μg/mL streptomycin, and 100 U/mL penicillin) was supplemented with 50 μg/mL ascorbic acid, 100 nM dexamethasone, and 5 mM β-glycerolphosphate. The polymers and polymer-coated NPs (prepared as described earlier) were dialyzed once more against high-glucose DMEM containing 100 μg/mL streptomycin and 100 U/mL penicillin. An aliquot of polymer or NP dispersion (10% of the final volume) was then incubated with the cells grown in 24-well tissue culture plates (in triplicate). After 72 h incubation in a humidified atmosphere with 95%/5% air/CO_2 at 37°C, 100 μL of the MTT solution (5 mg/mL in HBSS) was added to the 500 μL culture medium in each well. The cells were incubated for further 2 h, the supernatant was removed carefully, and 500 μL of dimethyl sulfoxide (DMSO) was added to the cells to dissolve the formazan crystals formed. The optical density of the solution was measured by an *EL*x800 plate reader (Bio-Tek Instruments Inc., Winooski, VT, USA) at 570 nm. Untreated cells served as reference and were taken as 100% viability.

BMP-2 bioactivity by kinetic ALP assay

A kinetic ALP assay was used to determine the bioactivity of BMP-2 encapsulated in the NPs. To prepare BMP-2 containing NPs, a certain amount of BMP-2 was first mixed with BSA solution, and then coacervated by acetone and coated with the polymers as described earlier. Following NP fabrication, all particles were dialyzed in the same manner as

described in the MTT procedure. Human C2C12 cells and rat BMSCs were incubated (in triplicate) with the NPs at the estimated concentration of 1 μg/mL of BMP-2 per well in 24-well plates (1 mL medium/well). The ALP assay was performed after the incubation of C2C12 cells for 3 days, and rat BMSCs for 7 days, based on optimal procedures developed in Wang et al. (2008). To perform the ALP assay, the cells were washed with HBSS solution and lysed with 400 μL of ALP buffer (0.5 M 2-amino-2-methylpropan-1-ol and 0.1% (v/v) Triton X-100; pH 10.5). After 2 h, 200 μL of 1.0 mg/mL ALP substrate (*p*-NPP) was added to 200 μL of the cell lysate, and the rate of change in the optical density was determined with a plate reader by measuring the absorbance (405 nm) at intervals of 90 sec for eight cycles. Untreated cells and cells treated with 1 μg/mL of free BMP-2 served as negative and positive controls, respectively. The kinetic ALP activity was expressed as the change of optical density of the wells per unit time (mAbs/min).

In vitro *HA affinity of BMP-2 containing NPs*

To determine the *in vitro* HA affinity of NPs, ^{125}I-labeled BMP-2 was encapsulated in the BSA NPs and the binding ability was assessed based on the ^{125}I counts. Labeling of BMP-2 with ^{125}I was performed as described previously (Gittens et al., 2004), and it was confirmed that the radioiodinated BMP-2 contained <4% free ^{125}I at the time of encapsulation. To prepare BMP-2 encapsulating NPs, ^{125}I-labeled BMP-2 (diluted in ddH_2O) was first mixed with BSA solution, and then coacervated by acetone and coated with the polymers by the evaporation method as described earlier.

The mineral affinity of the NPs was investigated by using a HA binding assay as described previously for the polymers. In this case, counts in the supernatant and HA precipitate were separately determined by a gamma counter. The percentage of HA-bound NPs (% HA binding) was calculated as follows: 100% × (count in HA precipitate)/(count in supernatant + count in HA precipitate).

In vivo *retention of BMP-2 encapsulated in NPs*

Six to eight weeks old female Sprague-Dawley rats were purchased from Biosciences (Edmonton, AB, Canada). The rats were acclimatized for 1 week under standard laboratory conditions (23°C, 12 h of light/dark cycle) before the study. While maintained in pairs in sterilized cages, rats were allowed free access to food and water for the duration of the study. All procedures involving the rats were approved by the Animal Welfare Committee at the University of Alberta.

The polymer-coated BSA NPs were prepared for implantation in 24 rats in four study groups. The study groups consisted of (1) BMP-2 in BSA solution, (2) BMP-2 in BSA NPs, (3) BMP-2 in PEI-PEG coated NPs, and (4) BMP-2 in PEI-PEG-thiolBP coated NPs. The appropriate solution for each study group was soaked into Skelite™ implants for ~10 min (50 μL of ^{125}I-labeled BMP-2 formulation per implant). The exact counts in the added 50 μL solution was determined by using a gamma counter and used as a measure of implanted BMP-2 dose. Once rats were anesthetized with inhalational Metofane™ (Janssen Pharmaceuticals Inc., Toronto, ON, Canada), two wet implants were implanted subcutaneously into bilateral ventral pouches in each rat. At indicated time points, two rats were euthanized with CO_2, the implants were recovered, and the counts associated with the excised implants were quantified by using a gamma counter. The amount of BMP-2 retention, expressed as the percentage of implanted dose, was calculated as follows: 100% × (recovered count in implant)/(initial count in implant). The results were summarized as mean ± SD (n = 4) of % BMP-2 retention in the implants at each time point.

Biodistribution of the BMP-2 containing NPs

The BSA NPs containing ^{125}I-labeled BMP-2 were prepared as previously described and 30 rats were utilized for the five study groups: (1) free BMP-2 in saline, (2) BMP-2 with BSA in saline solution, (3) BMP-2 in BSA NPs, (4) BMP-2 in PEI-PEG coated NPs, and (5) BMP-2 in PEI-PEG-thiolBP coated NPs. An aliquot of 300 μL of the sample was first counted by using a gamma counter to determine the injected dose, and then administered intravenously (IV) to the rats via tail vein injection over ~30 sec. The rats were killed at designed time points, long bones (tibia and femur), both kidneys, a portion of the liver, spleen, thyroid, and blood samples were collected, and counted by using a gamma counter. The biodistribution was analyzed based on the percentage of injected dose corrected according to the weight of the collected organs. Results are expressed as mean ± SD (n = 6 for femur, tibiae, and kidney, n = 3 for other tissues).

Statistical analysis

All experimental data were collected in triplicate at least, and expressed as mean ± standard deviations (SD). Statistical analysis was performed using two-sided unpaired Student's *t*-test or one-way ANOVA test. Differences were considered statistically significant with a *P*-value <0.05.

Results

Synthesis and characterization of PEI-PEG-thiolBP conjugate

The heterobifunctional NHS-PEG-MAL, which contains a thiol-reactive maleimide group and an amine-reactive NHS ester, was used for conjugating thiolBP onto PEI

(Scheme 1). ThiolBP was first coupled onto PEG to form NHS-PEG-thiolBP via the reaction between thiol group of thiolBP and the maleimide on NHS-PEG-MAL. Then, NHS-PEG-thiolBP was grafted onto PEI by reacting with primary amines of PEI. Successful grafting of NHS-PEG-MAL or NHS-PEG-thiolBP onto PEI was confirmed by ^{1}H-NMR (Figure 1). The extent of PEG grafting was determined from the relative peak area of –CH_2CH_2O– (δ: 3.64 ppm) of PEG to –CH_2CH_2N– (2.5–3.1 ppm) of PEI. Using a variety of PEG/PEI ratios up to 150:1, the results indicated that the substitution of NHS-PEG-MAL or NHS-PEG-thiolBP on PEI was comparable to the PEG/PEI feed ratio (data not shown). The appearance of peak at 1.88 ppm (–CH_2– of thiolBP) and the decrease or disappearance of maleimide signals at 5.85 and 6.25 ppm in ^{1}H-NMR spectrum (Figure 1B and C) indicated successful coupling of thiolBP to PEG-grafted PEI to some extent.

To obtain conjugates with different thiolBP substitutions, different concentrations of NHS-PEG-MAL was first reacted with excess thiolBP (thiolBP/PEG ratio of 1.5:1 and 4:1), and then reacted with PEI at PEG/PEI mole ratios of 10-150. As shown in Figure 2A, the thiolBP substitution efficiency was increased linearly from 5 to 24 thiolBP/PEI for feed ratio of thiolBP/PEG 1.5:1, as the PEG/PEI molar ratio was increased from 25 to 150, and from 7 to 33 thiolBP/PEI for feed ratio of thiolBP/PEG 4:1, as the PEG/PEI molar ratio increased from 10 to 50. This indicated that only a fraction of the thiolBP (<20%) was reacted with NHS-PEG-MAL and conjugated onto PEI branches. The obtained substitution pattern was similar to our previous study, where thiolBP was conjugated onto PEI using succinimidyl-4-(*N*-maleimidomenthyl) cyclohexane-1-carboxylate (SMCC) as the linker (Zhang et al., 2007).

In order to investigate the effects of PEG and thiolBP conjugation on the HA affinity of PEI, the HA affinity of PEI-PEG and PEI-PEG-thiolBP was examined in 0.1 M phosphate buffer (pH 7.4) and the results were summarized in Figure 2B. The unmodified PEI displayed significant HA affinity in phosphate buffer (>95% binding). The PEGylated PEI with low degree of substitution (<100 PEG/PEI) did not show significant loss in HA affinity, but at higher grafting ratio (>100 PEG/PEI), the ability to bind HA was reduced significantly ($P < 0.05$). However, the PEI-PEG-thiolBP conjugates recovered the mineral affinity (>97%) equivalent to unmodified PEI irrespective of the higher PEG substitution degree.

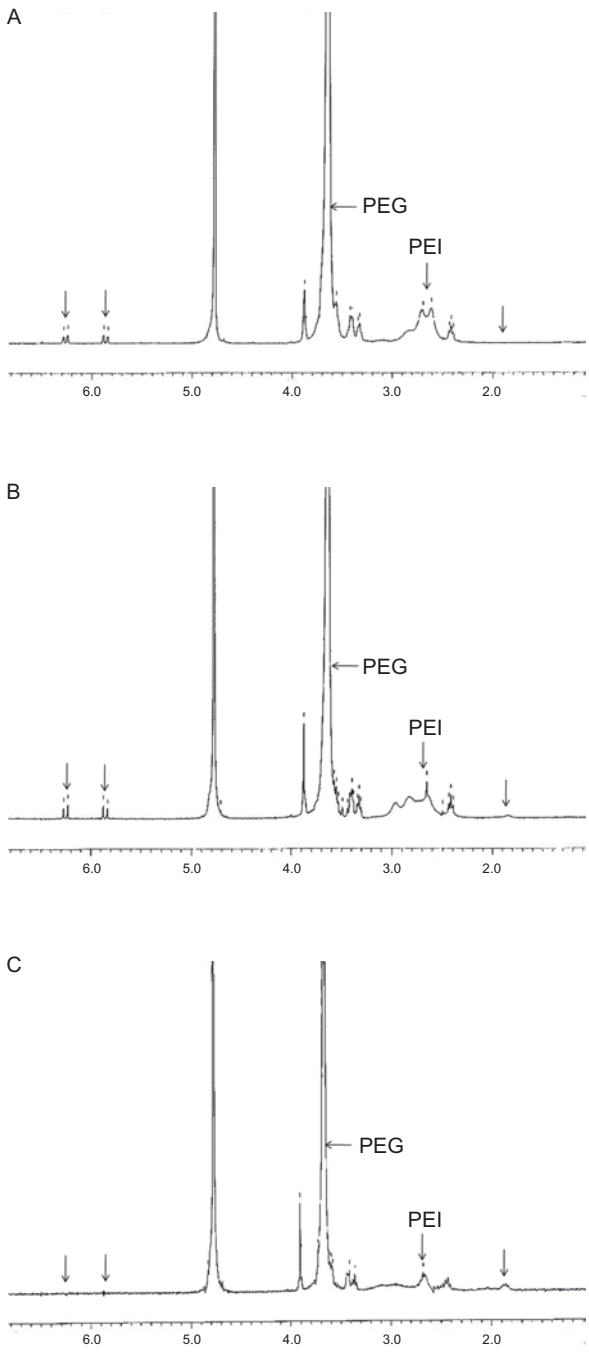

Figure 1. ^{1}H-NMR spectrum of PEI-PEG (A: 100 PEG per PEI) and PEI-PEG-thiolBP (B: 100 PEG and 18 thiolBP per PEI; C: 50 PEG and 33 thiolBP per PEI) in D_2O. The peak at 3.6 ppm was assigned to –CH_2CH_2O– from PEG, and the peaks at 2.5–3.1 ppm to –CH_2CH_2N– from PEI. Graft degree of PEG was determined from the relative peak area of PEG to PEI. Appearance of peak at 1.88 ppm (B and C) and disappearance of the maleimide peaks at 5.85 and 6.25 ppm (C) indicated that thiolBP was successfully conjugated to PEI.

Particle size and ζ-potential

The uncoated BSA NPs had a ζ-potential of –12.1 ± 2.7 mV in 1 mM NaCl. The ζ-potential of polymer-coated NPs gradually increased as a function of polymer/BSA ratio. This was the case whether dialysis (Figure 3A) or evaporation method (data not shown) was used for acetone removal. The ζ-potential of the PEI-coated particles reached to a plateau (~20 mV) above a certain concentration, which was consistent with our previous study (Wang et al., 2008; Zhang et al., 2008). Reaching a plateau value was indicative of the excess polymer in solution that was not bound to the NPs. The ζ-potential of PEI-PEG (150 PEG/PEI)

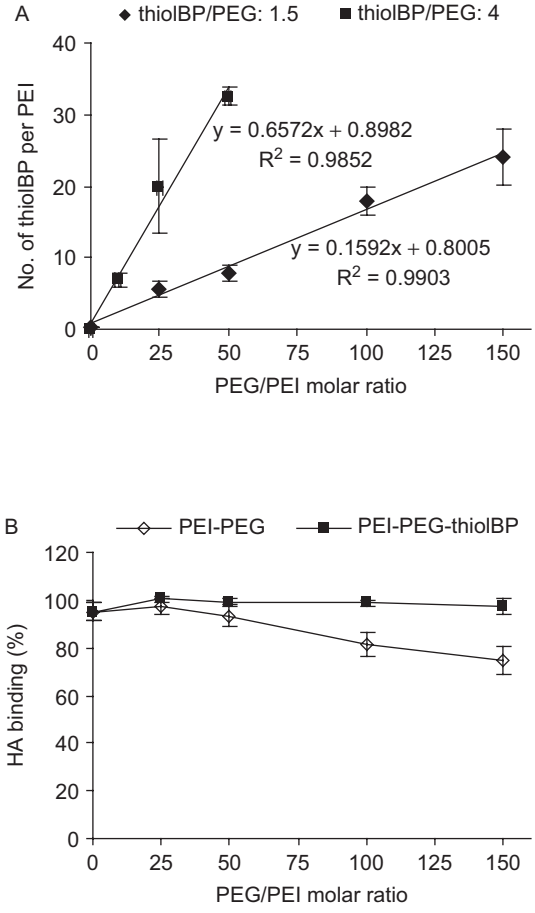

Figure 2. ThiolBP conjugation efficiency as a function of PEG/PEI molar ratio (A) and the influence of PEG substitution and thiolBP conjugation on HA affinity (B). The number of thiolBP per PEI was increased linearly from 6 to 24 as the PEG/PEI feed ratio increased from 25 to 150 for feed ratio of thiolBP/PEG 1.5:1 (diamond), and from 7 to 33 for feed ratio of thiolBP/PEG 4:1 as the PEG/PEI molar ratio increased from 10 to 50 (square). The PEG substitution on PEI led to reduced HA affinity at high PEG grafting, whereas the PEI-PEG-thiolBP conjugates displayed mineral affinity equivalent to unmodified PEI (0 PEG/PEI) at all PEG substitutions. Results are expressed as mean ± SD from three independent batches of experiments.

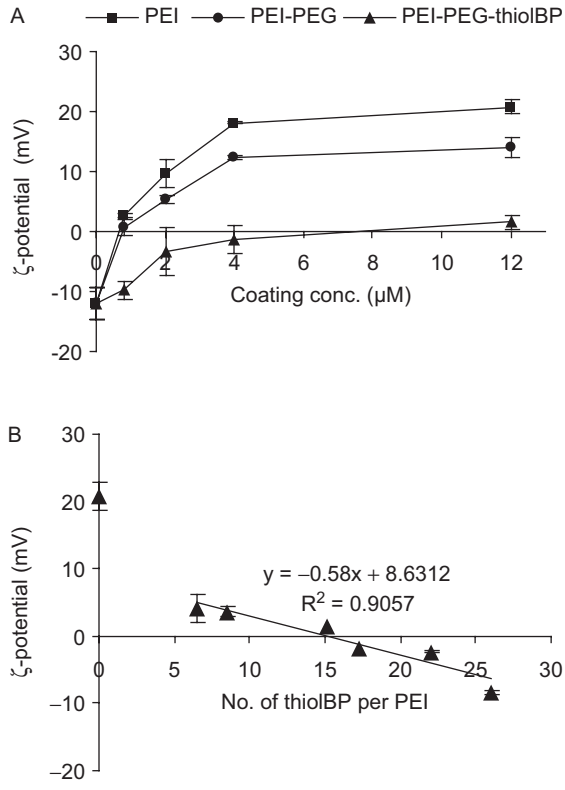

Figure 3. ζ-potential of BSA NPs coated by different concentrations of PEI, PEI-PEG, and PEI-PEG-thiolBP (0–12 μM) (A) and the effect of thiolBP substitution on PEI-PEG-thiolBP on ζ-potential of the NPs (B). The NPs were coated by the dialysis method. Results in (A) are expressed as mean ± SD from three independent binding experiment using PEI-PEG (150 PEG/PEI) and PEI-PEG-thiolBP (150 PEG and 24 thiolBP/PEI) for coating. Results in (B) are expressed as mean ± SD from triplicate measurements for the NPs coated by 4 μM of PEI-PEG-thiolBP with indicated numbers of thiolBP per PEI.

coated NPs decreased as compared with PEI coated NPs, having a maximum of ~14 mV. The PEI-PEG-thiolBP (24 thiolBP/PEI) reduced the ζ-potential more significantly and eventually maintained the NPs at neutral ζ-potential after 4 μM or higher coating concentration. Using a range of PEI-PEG-thiolBP conjugates with different extent of thiolBP conjugation, the ζ-potential was found to inversely depend on the thiolBP substitution (Figure 3B); at 4 μM coating concentration, the conjugates with higher thiolBP substitution led to lower ζ-potential.

Two methods used to prepare the polymer-coated BSA NPs were compared with respect to the obtained particle sizes and size distributions (Figure 4). The size of NPs suspended in acetone/water was 43.7 ± 4.6 nm, and narrowly distributed, with a polydispersity index (PDI) of 0.105 ± 0.059 in diameter. After removing the acetone by dialysis, the zeta-average size and PDI of uncoated NPs were increased to 157.6 ± 21.8 nm and 0.463 ± 0.013, respectively. The PEI-PEG-thiolBP coated NPs had a size of 130.6 ± 13.9 nm, and PDI of 0.365 ± 0.095. Both the uncoated and coated NPs displayed two separate peaks for the size distribution, the left one (peak 1) being ~60 nm and the right one (peak 2) >200 nm (Figure 4B and C), indicating the presence of large aggregates in the samples. For the evaporation method, the average sizes of the uncoated and coated NPs were 117.5 ± 5.3 nm and 77.3 ± 2.0 nm, respectively, which were smaller than their counterparts from the dialysis method. For the coated NPs, although there was a decrease for zeta-average size from the dialysis method to evaporation method, the mean size of the single peak in Figure 4E was comparable to the first peak in Figure 4C. The peak in the larger size range disappeared for the evaporation method, which indicated no aggregates for the PEI-PEG-thiolBP coated BSA NPs.

The sizes of the NPs obtained as a function of coating concentration by dialysis method are summarized in

A

NPs	Particle size[a] (nm)	PDI[a]	Peak 1[b]		Peak 2[b]	
			Area (%)	Mean (nm)	Area (%)	Mean (nm)
BSA NP in acetone/water	43.7 ± 4.6	0.105 ± 0.059	100	42.7		
Dialysis method						
Uncoated BSA NPs	157.6 ± 21.8	0.463 ± 0.013	67.5	64.0	32.5	290.7
PEI-PEG-thiolBP coated NPs	130.6 ± 13.9	0.365 ± 0.095	85.9	57.3	14.1	395.1
Evaporation method						
Uncoated BSA NPs	117.5 ± 5.3	0.676 ± 0.037	90.7	56.7	9.3	458.9
PEI-PEG-thiolBP coated NPs	77.3 ± 2.0	0.376 ± 0.025	100	57.9		

a: results are expressed as mean ± SD (zeta-average) from three independent batches of NPs.

b: data are taken from a typical measurement for each formulation.

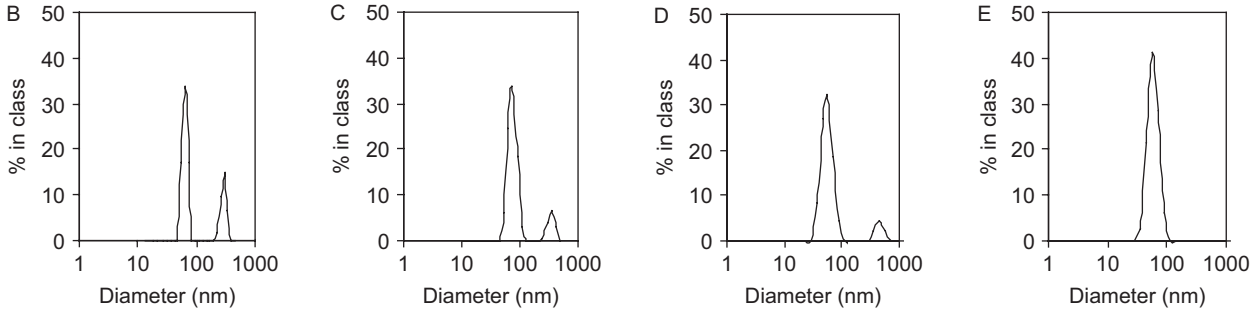

Figure 4. Particle size analysis (A) and size distributions of uncoated BSA NPs (B, dialysis method; D, evaporation method) and PEI-PEG-thiolBP (4 μM) coated NPs (C, dialysis method; E, evaporation method). Note that obvious aggregation existed for the uncoated BSA NPs in (B) and (D), and the PEI-PEG-thiolBP coated NPs by dialysis method (C), whereas the coated NPs by evaporation method (E) displayed a narrow single peak.

Figure 5. Using a PEI-PEG with 150 PEG/PEI, the mean size showed a dramatic change as a function of polymer concentration, an increase up to ~380 nm for the lowest coating concentration (1 μM) and followed by a decrease to ~200 nm for 2 μM coating and a plateau of ~150 nm at >4 μM. The sizes of PEI-PEG-thiolBP coated NPs (24 thiolBP/PEI) increased slightly for the lowest concentration and then maintained at ~130 nm.

The NPs were analyzed by AFM to confirm the size of the particles measured by PCS. As shown in Figure 6, the BSA NPs in acetone/water were uniform with the size of ~50 nm, and generally spherical with smooth surface characteristics. The PEI-PEG-thiolBP coated NPs from the evaporation method showed a particle size of 50–70 nm, relatively rougher surfaces with no visible aggregates. The size of coated NPs obtained from these images was slightly smaller than that from PCS analysis, which was possibly due to the shrinkage of the particles during the drying process for the AFM sample preparation.

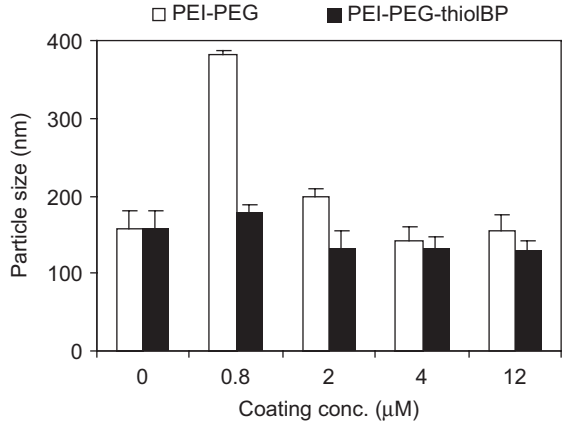

Figure 5. Effect of coating concentration on particle size of polymer-coated BSA NPs. The NPs were prepared by dialysis method with 0–12 μM of PEI-PEG (150 PEG/PEI) or PEI-PEG-thiolBP (150 PEG and 24 thiolBP/PEI). Results are expressed as mean ± SD from three independent batches of NPs.

Cytotoxicity

Two types of cells, myogenic C2C12 cells and rat BMSCs, were used to assess the relative toxicity of the polymer conjugates (Figure 7A and B, respectively) and the polymer-coated NPs (Figure 7C and D, respectively). As shown in Figure 7A, the polymers did not show any toxicity on C2C12 cells at <4 μM. However, cell viability was significantly ($P < 0.05$) decreased at higher PEI

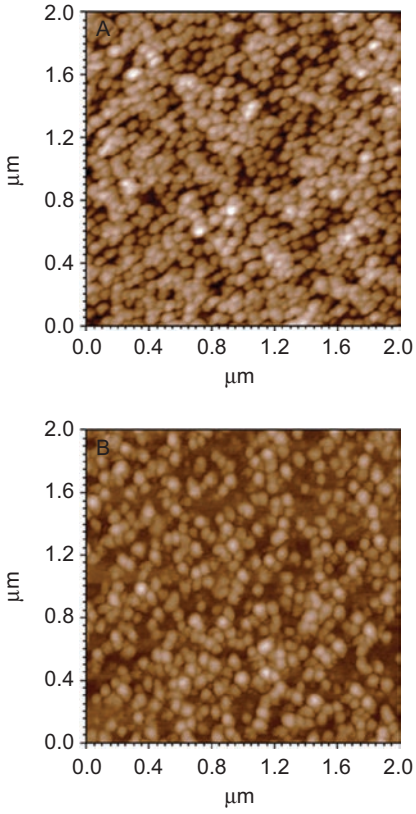

Figure 6. AFM images of BSA NPs in acetone/water (A) and PEI-PEG-thiolBP coated BSA NPs (B) prepared by using evaporation method for coating. The images are 2 × 2 µm in scale and representatively selected from a large series of images generated from AFM.

concentrations (>8 µM) with >70% loss of cell viability. Conversely, PEI conjugates with PEG did not exhibit any cytotoxicity at a concentration of 8 µM, and it showed significantly improved cell viability as compared with PEI ($P < 0.05$) at the highest concentration tested. The incorporation of thiolBP did not impart any additional toxicity on the PEI-PEG. The cytotoxicity of the polymers on rat BMSCs (Figure 7B) displayed a pattern similar to that of C2C12 cells, where PEI was found to be most toxic, and thiolBP conjugation to PEG did not cause any additional toxicity, except for a slight loss of viability at higher concentrations compared with the control.

The effects of polymer coating on NP toxicity were investigated after coating the NPs with PEI, PEI-PEG (150 PEG/PEI) and PEI-PEG-thiolBP (24 thiolBP/PEI-PEG). As shown in Figure 7C, only the PEI-coated NPs at the highest concentration (12 µM) displayed significant toxicity on C2C12 cells. There was no significant difference in cell viability for NPs coated with PEI-PEG and PEI-PEG-thiolBP. For rat BMSC, the highest concentration of PEI (12 µM) showed significant toxicity again. Different from the C2C12 cells, the uncoated NPs showed some toxicity (~20% decrease in viability), and all polymer coated NPs showed a further 10–20% decrease in cell viability ($P < 0.05$; Figure 7D). Nevertheless, PEG substitution on PEI reduced PEI toxicity at high concentration and the toxicity of the PEI-PEG or PEI-PEG-thiolBP coated NPs were considered tolerable for *in vivo* studies.

Bioactivity of encapsulated BMP-2

The change of ALP activity is a well-demonstrated hallmark of osteogenesis phenomena in physiological tissues or cells. Myogenic C2C12 cells (Zhang et al., 2008) and rat BMSCs (Varkey et al., 2006) both display stimulated ALP induction as a result of BMP-2 treatment. In this study, we utilized both types of cells to evaluate the bioactivity of NP-encapsulated BMP-2, and the results were summarized in Figure 8. The exact contents of BMP-2 in NPs were not determined in this study. We assumed full retention of BMP-2 amount in the NPs, based on our previous study (Zhang et al., 2007), which indicated >90% encapsulation efficiency, and tested our NP-encapsulated BMP-2 against an equivalent amount of free BMP-2. For the C2C12 cells (Figure 8A), no activity was noted for the untreated cells after 3 days incubation. All NP-encapsulated BMP-2 showed significant ALP activity, and the numbers were equivalent to or higher than the cells treated with free BMP-2, except for the NPs coated with highest concentration of PEI, which might have induced some toxicity to the cells. Different from the C2C12 cells, the untreated rat BMSCs (Figure 8B) showed a strong background in ALP activity, whereas all NP-encapsulated BMP-2 formulations showed significant increase in ALP activity on day 7 ($P < 0.05$ compared with untreated control), which were equivalent to free BMP-2.

Bone mineral affinity of polymer-coated NPs

The mineral affinity of different NPs was investigated both *in vitro* and *in vivo*. For *in vitro* study, the extent of the polymer-coated NP binding to HA was determined after encapsulating ^{125}I-labeled BMP-2 in the NPs. As shown in Figure 9A, the free BMP-2 could adsorb onto the HA by itself to some extent (~60%) either in water or in 0.1 M phosphate buffer (pH 7.4). All NP-encapsulated BMP-2 evaluation displayed a higher HA affinity (~90%) in both buffers. The binding assay did not indicate any significant difference in HA affinity among the NPs investigated.

The *in vivo* mineral affinity was also examined in a rat subcutaneous implant model (Figure 9B and C). Commercially available Skelite™, a microporous scaffold used in clinical osteoconductive bone repair, was used as an implant. ^{125}I-labeled BMP-2 was used to determine the retention of NPs in the implants. In one batch of NPs (Figure 9B), the retention of free BMP-2, BMP-2 encapsulated in BSA NPs, PEI-PEG coated NPs, and PEI-PEG-thiolBP coated NPs after 2 days implantation were 51.2 ± 3.4%, 66.3 ± 6.7%, 73.8 ± 7.9%, and 83.3 ± 4.5%, respectively. The PEI-PEG-thiolBP coated NPs displayed

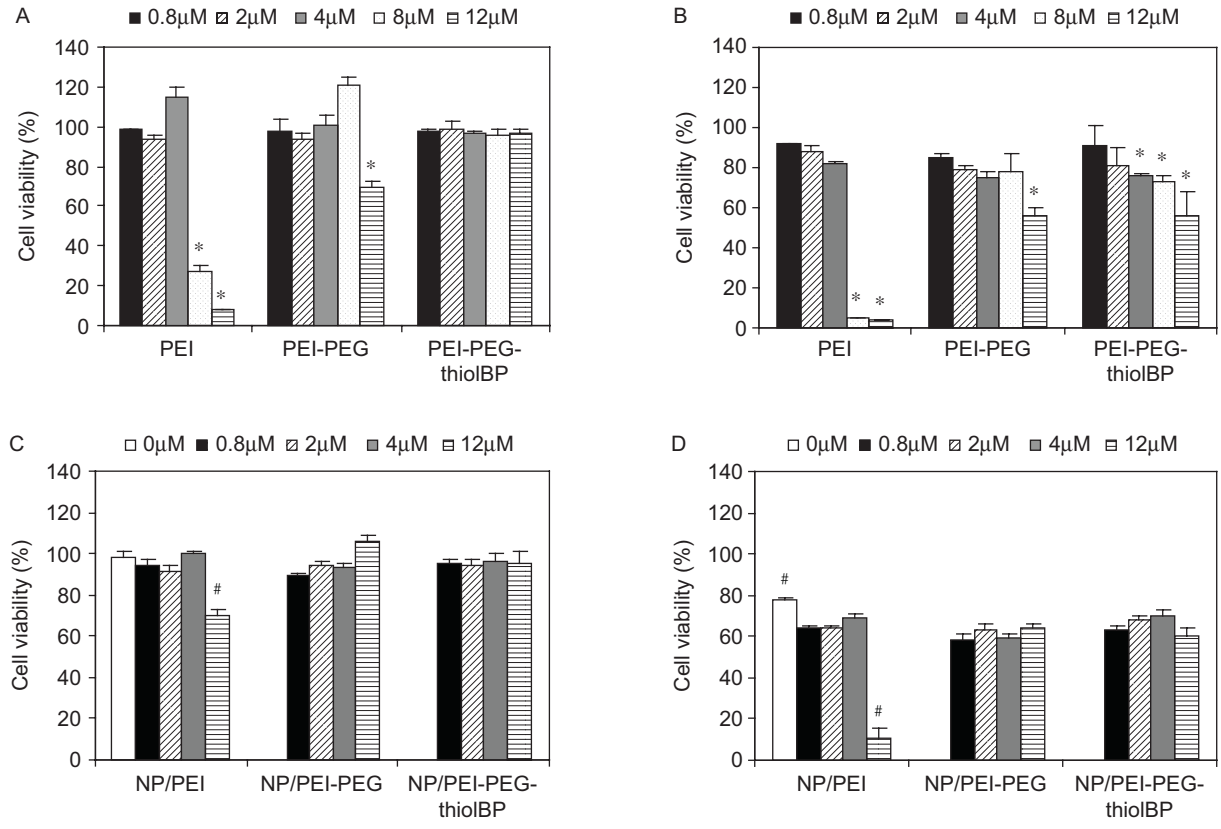

Figure 7. Cytotoxicity of polymer conjugates on (A) C2C12 cells, and (B) rat BMSCs, and polymer-coated BSA NPs on (C) C2C12 cells, and (D) rat BMSCs. The conjugates used for coating were 150 PEG/PEI for PEI-PEG, 150 PEG, and 24 thiolBP/PEI for PEI-PEG-thiolBP). The concentrations shown were equivalent to the polymer concentrations used for coating the BSA NPs. Untreated cells served as reference and were taken as 100% viability. Results are expressed as mean ± SD from triplicate wells. Statistically significant ($P < 0.05$) groups compared to control (*) and other groups (#) are indicated.

enhanced BMP-2 retention compared to the free BMP-2 and uncoated BSA NPs ($P < 0.05$). For another batch (Figure 9C), after 2 days, the retention of free BMP-2 (in BSA solution) was 37.4 ± 3.4%, while the BMP-2 retention in uncoated, PEI-PEG coated and PEI-PEG-thiolBP coated BSA NPs were 55.4 ± 4.9%, 64.8 ± 4.0%, and 72.2 ± 3.0%, respectively. At day 10, the retention of BMP-2 for the latter three groups were 33.0 ± 6.5%, 43.7 ± 7.4%, and 39.7 ± 8.7%, while that of free BMP-2 was 20.0 ± 3.5%. During the study period, the BMP-2 retention in the three NP formulations was significantly higher than free BMP-2 ($P < 0.05$), but only at day 2, the PEI-PEG-thiolBP coated NPs showed significantly improved BMP-2 retention than the uncoated ones ($P < 0.05$). The PEI-PEG-thiolBP coated BSA NPs had slightly higher BMP-2 retention than PEI-PEG coated ones till day 7, and lower at day 10, but the difference between the two groups was not significant ($P > 0.05$).

Biodistribution of the BMP-2 containing NPs

To determine the feasibility of targeting NPs to bones, the NP formulations prepared with ^{125}I-labeled BMP-2 were intravenously injected in rats via tail vein, and analyzed for biodistribution at day 1 and day 4 after injection (Figure 10A and B). Thyroid had the highest uptake of radioactivity after 24 h where 10–25% of the injected dose was localized. This was ~100 times higher than the deposition at other organs and reflected the presence of free iodine in circulation. Kidney, liver, and spleen also showed obvious uptake except for the uncoated BSA NPs in spleen. The retention of the BMP-2 in blood after one day injection was drastically depressed (<0.02%). Although both the *in vitro* and *in vivo* binding results showed improved HA affinity for the NP-encapsulated BMP-2 as compared with free BMP-2, the NPs did not indicate any superior bone-targeting (<0.03% for all groups), and there was no significant difference in bone (femur and tibiae) deposition of the NPs. Instead, the PEI-PEG and PEI-PEG-thiolBP coated BSA NPs had a significantly higher deposition in spleen compared with the uncoated ones.

Similar experiments were performed independently with NPs coated with thiolBP and alendronate (after thiolation) conjugate of PEI-PEG; however, the results were essentially the same as before (data not shown), and no beneficial effects were noted on bone deposition for any of the BP-coated NPs.

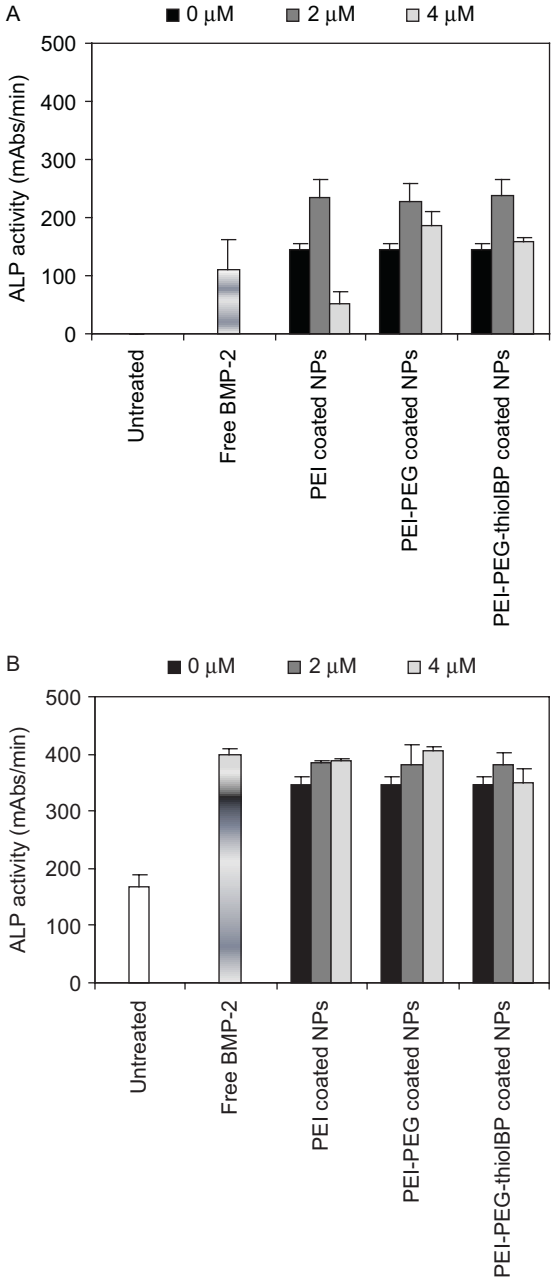

Figure 8. ALP activity of NP-encapsulated BMP-2 on (A) C2C12 cells and (B) rat BMSCs. Results are expressed as mean ± SD from triplicate wells. The conjugates used for coating were 150 PEG/PEI for PEI-PEG, 150 PEG, and 24 thiolBP for PEI-PEG-thiolBP. The concentrations shown were equivalent to the polymer concentrations used for coating the BSA NPs. All the NP-encapsulated BMP-2 showed equivalent or highest ALP activity compared to free BMP-2, except for the C2C12 cells treated with NPs coated with higher concentration of PEI.

Discussion

Coupling of thiol group to maleimide is a convenient method for PEG conjugation to thiolBP, as the reaction is site-specific, easy to control, and leads to a stable 3-thiosuccinimidyl ether linkage. Since branched PEI contains a combination of primary, secondary, and tertiary amines, and 31% of the amino groups (~180 for 25 kDa PEI) are primary amines (von Harpe et al., 2000), ample PEG chains can be coupled to PEI via the amine-reactive NHS ester. A stoichiometric reaction between the NHS-PEG-MAL and PEI at their predetermined molar ratios was reported previously (Tang et al., 2003). In this study, we also observed 100% conjugation efficiency of NHS-PEG-MAL or NHS-PEG-thiolBP to PEI. Although the ^{1}H-NMR spectrum confirmed successful conjugating of thiolBP to PEG-grafted PEI, the relevant signals of thiolBP and maleimide were much weaker than the broad H-signals of PEG and PEI residues, which made it difficult to accurately calculate the thiolBP content in the samples. Therefore, the conjugation efficiency of thiolBP was based on organic phosphate assay and it was found to be relatively lower than expected, which was likely due to the formation of disulfides among thiolBPs, leading to the reduction of available free thiols. Therefore, excess thiolBP was needed for saturation of the maleimide on the PEG.

We previously reported on PEI-coated BSA NPs, and observed cationic particles with size >200 nm (Wang et al., 2008; Zhang et al., 2008). The size and surface charge of the NPs were expected to decrease by using PEG-substituted PEI as a result of surface shielding by PEG. As in our previous studies, physical adsorption was suitable for coating NPs with PEG-modified polymers given the cationic backbone in these polymers. The positively charged PEI backbone was expected to bind on NP surfaces, whereas the PEG and thiolBP chains to extend to the NP exterior. The hydrophilic PEG surface not only screened the highly positive charge of the adsorbed PEI, but also effectively stabilized the BSA NPs by reducing particle aggregation. The negatively charged thiolBP made the NPs coated with PEI-PEG-thiolBP display a low ζ-potential. Under this circumstance, neutral particles usually show a tendency to agglomerate. Even though PEI-coated cationic surfaces were expected to reduce NP aggregation, PEI-PEG-thiolBP coating resulted in smallest particles despite having almost neutral surfaces. The presence of the surface PEG chains might have prevented aggregation by a steric repulsion mechanism.

Since the particle sizes from PCS measurement were analyzed based on the seventh moment of diameter (Finsy & De Jaeger, 1991), it might be extremely sensitive to the presence of any larger aggregates, which was evident in some samples (Figure 4). For example, <10% of larger particles can increase the zeta-average size of uncoated NPs prepared by evaporation method from <60 nm to >100 nm. As shown in Figure 4A, the PDI of the different NPs was typically higher than 0.3, which indicated that the NP dispersions were somewhat polydispersed. The appearance of two peaks in size distributions indicated obvious aggregates. For the dialysis method, the coating

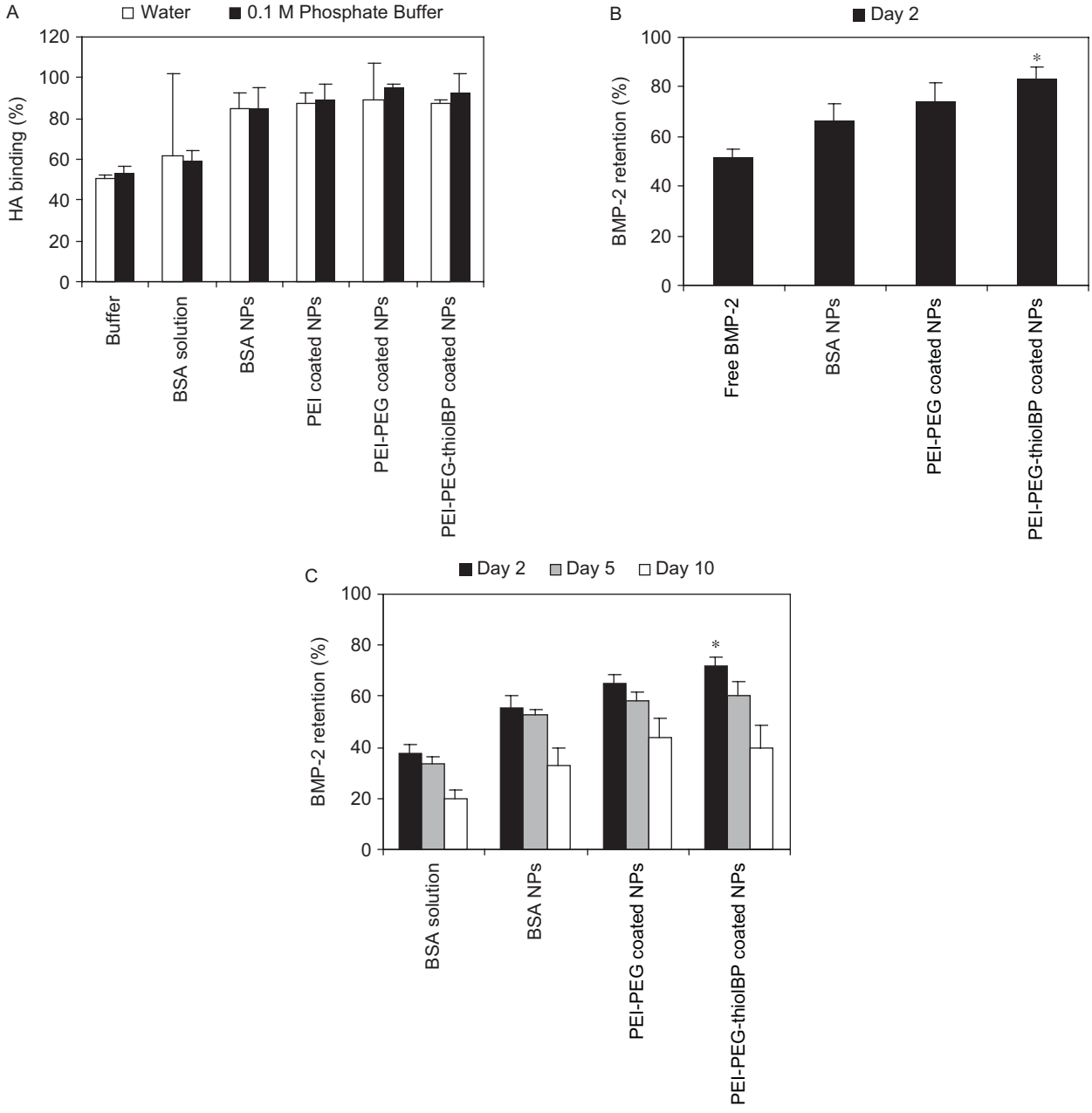

Figure 9. *In vitro* HA affinity (A) and *in vivo* implant retention (B, Day 2; C, Day 2–10) of ^{125}I-labeled BMP-2 in different NP formulations. The *in vitro* binding was performed in either ddH_2O or 0.1 m phosphate buffer (pH 7.4). All NPs displayed higher HA binding and *in vivo* retention of NP-encapsulated BMP-2 than the free BMP-2 and BMP-2 in BSA solutions ($P < 0.05$). However, no difference was seen among the HA affinity of various NPs *in vitro* (A). In the implant model (B and C), PEI-PEG-thiolBP coated NPs showed the highest retention among all NP formulations until day five post-implantation ($P < 0.05$ vs. free BMP-2 and uncoated NPs), though there was no significant difference from the PEI-PEG coated NPs ($P > 0.05$). At day 10, the BMP-2 retention was decreased for all groups, and the coated NPs retained the highest amount of BMP-2 (>40%) in implants ($n = 4$ implants at each time point).

of PEI-PEG-thiolBP decreased the extent of aggregation (peak 2 area decreased from 32.5% to 14.1%), but could not completely prevent it. The evaporation method was advantageous for this purpose by displaying only a single peak at <60 nm. Compared with the BSA NPs in acetone/water, the uncoated BSA NPs after removing acetone was 15–20 nm larger (peak 1), which was likely due to the swelling of the particles. However, after adsorbing a layer of PEI-PEG-thiolBP, which has a coiled PEG chain less than 10 nm in length (Garbuzenko, Barenholz, & Priev, 2005), their sizes remained comparable to those in the acetone/water coacervation system. The unchanged sizes of NPs even after coating implied that ionic anchoring of the positively charged conjugate on the negatively charged surface might prevent NPs from swelling and aggregating after removing the coacervation agent acetone.

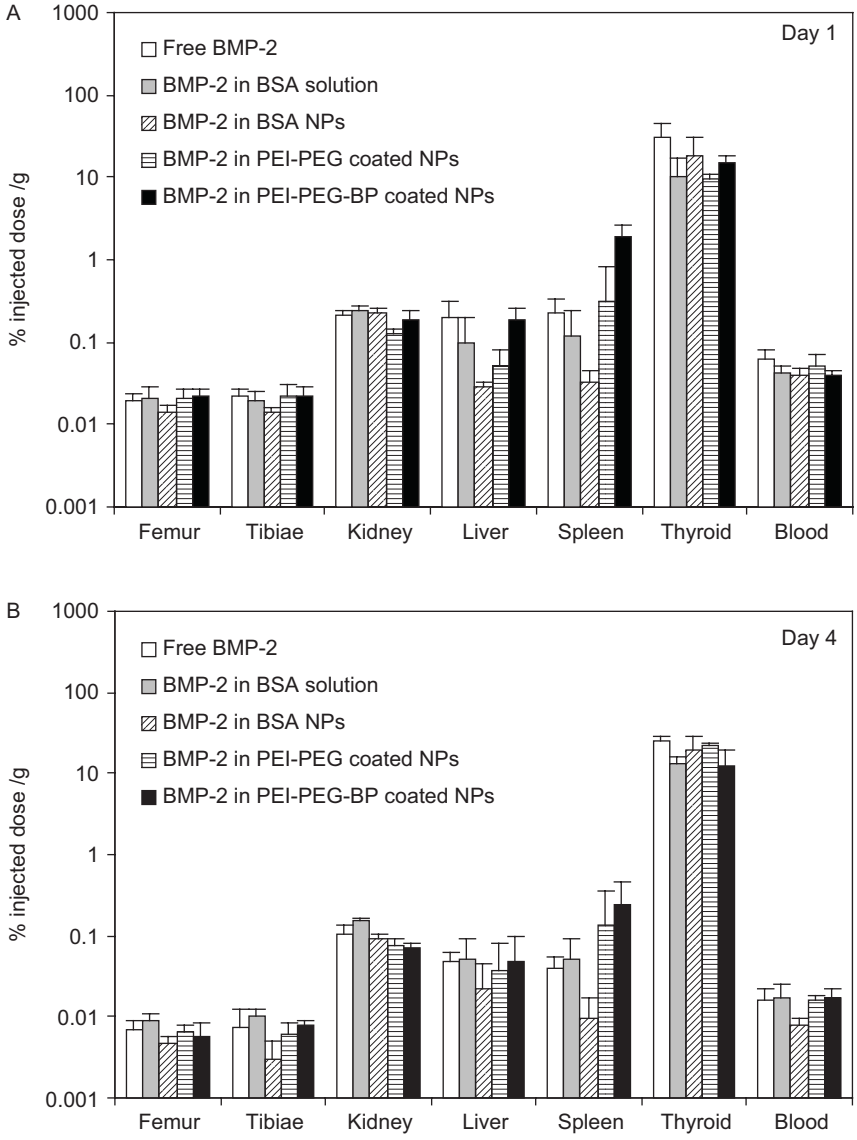

Figure 10. The biodistribution of ^{125}I-labeled BMP-2 encapsulated in different BSA NPs. The samples were administered intravenously to the rats by tail vein injection, and the biodistribution was analyzed at (A) day 1 and (B) day 4 after injection. Results (% injected dose) are expressed as mean ± SD ($n = 6$ for femur, tibiae, and kidney, $n = 3$ for other tissues) and normalized with the weight of the tissue (g).

Significant toxicity is well established for PEI with high molecular weight (Godbey, Wu, & Mikos, 2001), although the reasons for PEI toxicity are not completely clear. PEGylation of PEI effectively reduced the toxicity of PEI, and this was likely due to the shielding effects on the net charge of the PEI backbone. Two types of cells were used in this study to test the toxicity of the polymer and particles. C2C12 cells are particularly suitable for assessing BMP-2 activity, whereas they are more robust than primary cells and their BMP-2 response is more predictable. BMSCs derived from rats were also used since the intended use of our formulations is to deliver BMP-2 and one of the primary targets of BMP-2 is stem cells at the bone marrow environment. Both the C2C12 cells and BMSCs indicated reduced PEI toxicity after PEG substitution. In our recent study, the potential of using BSA NPs for localized bone regeneration was affirmed, and the PEI coating on the BSA NPs displayed improved BMP-2 retention in implant. However, the surface coating of PEI at higher concentrations impaired the efficacy of BMP-2 to induce bone formation in a rat subcutaneous model (Zhang, Doschak, & Uludag, 2009). The reduced toxicity of PEGylated PEI might be alternative for future study.

Maintenance of the native bioactivity of an osteogenic growth factor is essential for a NP formulation designed for local or systemic administration of growth factor. Our previous study (Wang et al., 2008) indicated that PEI and PLL coated BSA NPs can fully retain the BMP-2 activity after encapsulation. PEI was shown to be a relatively toxic

component of the NPs (Zhang et al., 2009), but PEG substitution on PEI was shown to reduce toxicity when this polymer was used for NP coating (Zhang et al., 2010). In this study, we further evaluated the effect of BP modification of NPs on the activity of encapsulated BMP-2. The myogenic cells (C2C12 cells) showed a significant BMP-2 activity with the NPs decorated with thiolBP, which confirmed there was no adverse effect of the presence of BPs on BMP-2 induced osteogenesis response. The positive effects with the primary cells (rat BMSCs), which are directly relevant to physiological osteogenesis, also provide encouraging prospect for *in vivo* testing of the proposed NPs. Direct measurement of BMP-2 release from the NP formulations were not performed in this study. Based on previous results (Zhang et al., 2009), we anticipate most BMP-2 (>50%) to be released from the NPs in 1 week time under the cell culture conditions. Whether the NPs are internalized or whether the internalized BMP-2 exerts a significant bioactivity remain to be investigated.

The BPs are commonly used for the inhibition of osteoclast activities, and known for their unique pharmacokinetic and biodistribution profiles favoring fast deposition and long residence in the skeleton tissues. Bone-targeted delivery of NPs has been attempted by several groups based on BP molecules. Choi and Kim (2007) conjugated alendronate to PLGA NPs via PEG-PLGA block copolymers and found that alendronate-modified NPs had a strong and specific adsorption to HA, and the potency of HA adsorption was dependent on the content of alendronate and the block length of PEG. PEI itself displays significant interaction with charged surfaces (Radeva & Petkanchin, 1997; Meszaros et al., 2002), and our previous study also indicated a high affinity of PEI to bone mineral HA (Zhang et al., 2007). However, when conjugated with PEG, which has a negative effect on surface adsorption and HA affinity (Wang et al., 2003, 2005), the PEG modified PEI dramatically decreases its inherent ability of binding to HA as a function of PEG substitution degree. The loss of HA affinity caused by PEG substitution could be offset via the further conjugation with BP. This was confirmed by our results, which indicated that the HA binding ability of PEI-PEG was decreased gradually from 95% of pure PEI to 75% for PEI-PEG with 150 PEG per PEI, whereas the PEI-PEG-thiolBP remained >97% HA binding regardless the PEG substitution degree.

The excellent HA affinity of PEI-PEG-thiolBP makes this polymer potentially suitable to target therapeutic agents to the bone, besides the advantages discussed earlier with respect to non-aggregation, masked surface charge, and reduced toxicity. However, such an affinity should be retained after the PEI conjugates are adsorbed onto the NPs. From the HA binding results, all NPs displayed higher percentage of NP binding to the HA as compared with free BMP-2, but the polymer-coated NPs did not show any improvement in the HA affinity compared with the uncoated ones. However, the *in vivo* BMP-2 retention study showed superiority of the NPs coated with PEI-PEG-thiolBP, which gave higher retention at specific time points. On one hand, these results suggest that *in vivo* HA affinity by BP-conjugated NPs is better revealed. On the other hand, the differences between PEI-PEG and PEI-PEG-thiolBP were not as strong as expected, and might indicate that mineral affinity of the formulations was likely dominated by the same factors. Nevertheless, the improved retention of BP-decorated NPs in mineral-rich scaffolds suggests that the prepared NPs might provide a potential candidate for localized delivery system of BMP-2 for bone repair and regeneration when administered locally with mineral-based scaffolds.

No beneficial effects of polymer coating was noted for NP targeting to bones after IV administration, despite strong evidence for NP binding to HA *in vitro*. The reasons for this observation remain to be elucidated. The organ accumulation of BMP-2 after 1 and 4 days of IV administration was estimated by assuming that the ^{125}I-labeling was stable on the protein *in vivo*. The distinct thyroid uptake (~100 times higher than other organs) of radioiodine indicated a significant de-iodination of the ^{125}I-labeled BMP-2 during the study. It was reported that free iodine formed by rapid de-iodination of the radioiodinated proteins accumulated mainly in thyroid, stomach, lung, or spleen (Lin et al., 2009). However, this unavoidable artifact was not an impediment for the use of ^{125}I labeling in studying protein targeting to bones, and should not be the reason for the lack of bone targeting observed in this study.

In vivo deposition of particles to hard tissue is more complicated than retention in implants and requires a long blood circulation time and site-specificity. A hydrophilic surface and small particle size (<100 nm) are expected requirements to avoid the reticuloendothelial system (Choi & Kim, 2007). The coating with PEI-PEG was designed for this purpose, and the size measurements indicated that the PEI-PEG-thiolBP coated BSA NPs (77 nm) exhibited hydrophilic surfaces. However, it is known that the fenestrated capillaries or sinusoids in the bone have pores of 80–100 nm (Tye et al., 2003). In order to extravasate and deposit in bones, the hydrodynamic diameters of the NPs should be <80 nm. The sizes of the smallest BSA NPs investigated in this study was close to 80 nm; thus, the extravasation of these particles into the bone fluid might have been hampered. Other factors affecting biodistribution of NPs include surface properties, which are directly correlated to the interactions between the particles and components in the physiological fluid. It is reported that negative charges influence the clearance of the particles from the blood circulation via kidney glomerular filtration and liver uptake (Moghimi,

Hunter, & Murray, 2001). The low surface charge of the PEI-PEG-thiolBP coated NPs might be also a factor influencing the capture of these NPs by cells of the monocyte-macrophage system (mainly the liver and spleen). The saturated calcium and iron ions in blood may bind to the BP-conjugated macromolecules to form chelate complex (Uludag, 2002), which would presumably be removed faster by the clearance organs. The strength and stability of non-covalent binding of polymers to a NP surface might be another issue. In circulation, the surface adsorbed polymers might dissociate from the NP surface and/or get displaced by plasma proteins, which may make the particles prone to phagocytosis. Even for the stably adsorbed polymers, the chemical breakdown processes of the polymeric texture, such as swelling, degradation, and erosion, may decrease the steric shielding effect and induce surface changes favorable for opsonization, leading to uptake by RES. Salts and proteins in the serum may induce disassociation of surface coating and/or *in vivo* aggregation, which might also affect the biodistribution of the NPs.

In conclusion, thiolBP- and PEG-modified PEI was used to decorate BSA NPs to tune their particle size and surface charge, reduce the PEI toxicity, and improve their HA affinity. The polymer coating and BP decoration had no adverse effect on the bioactivity of the NP-encapsulated BMP-2. All the NPs displayed significant *in vitro* HA affinity and *in vivo* retention for encapsulated BMP-2. The BP-conjugated NPs, with enhanced *in vivo* retention in mineral implants, are potential candidate for localized delivery system of BMP-2 for bone repair and regeneration. However, when administered intravenously, no beneficial effects were observed for the thiolBP-coated BSA NPs on the bone-targeting. Although successful targeting of BP-conjugated copolymer to bone was reported (Wang et al., 2003), NPs prepared with BPs were only tested in *in vitro* HA binding (Hengst et al., 2007; Choi & Kim, 2007; Anada et al., 2009; Pignatello et al., 2009), and none of these studies reported bone targeting *in vivo*. This includes several patents, which showed superior hydroxyapatite affinity of BP-derivatized NPs, but provided no results on the feasibility of bone targeting by such NPs (Vail). To the best of our knowledge, this study was the first to report the evaluation of *in vivo* bone targeting of BP-modified NPs, and the unsuccessful outcome calls for better understanding of the *in vitro* behavior of BP-decorated NPs with the hope of designing bone-seeking NPs.

Acknowledgements

This project was funded by an operating grant from the Canadian Institutes of Health Research (CIHR). Guilin Wang is supported by studentships from the China Scholarship Council (CSC) and a CIHR Skeletal Regenerative Medicine Team grant (PI: D.E. Rancourt, University of Calgary). The BMP-2 was kindly provided by Dr Walter Sebald (University of Wurzburg, Germany). The authors thank Dr Hamid Montazeri for technical help with IV injection.

Declaration of interest

The authors report no conflicts of interest. The authors alone are responsible for the content and writing of the paper.

References

Ames BN. (1966). Assay of inorganic phosphate, total phosphate and phosphatases. In: *Methods in Enzymology. Neufeld EF*, Ginsburg V (eds). New York: Academic Press, pp. 115–117.

Anada T, Takeda Y, Honda Y, Sakurai K, Suzuki O. (2009). Synthesis of calcium phosphate-binding liposome for drug delivery. Bioorg Med Chem Lett, 19, 4148–4150.

Bansal G, Gittens SA, Uludag H. (2004). A di(bisphosphonic acid) for protein coupling and targeting to bone. J Pharm Sci, 93, 2788–2799.

Bansal G, Wright JE, Zhang S, Zernicke RF, Uludag H. (2005). Imparting mineral affinity to proteins with thiol-labile disulfide linkages. J Biomed Mater Res A, 74, 618–628.

Bronich TK, Cherry T, Vinogradov SV, Eisenberg A, Kabanov VA, Kabanov AV. (1998). Self-assembly in mixtures of poly(ethylene oxide)-graft-poly(ethyleneimine) and alkyl sulfates. Langmuir, 14, 6101–6106.

Bullock J, Chowdhury S, Severdia A, Sweeney J, Johnston D, Pachla L. (1997). Comparison of results of various methods used to determine the extent of modification of methoxy polyethylene glycol 5000-modified bovine cupri-zinc superoxide dismutase. Anal Biochem, 254, 254–262.

Choi SW, Kim JH. (2007). Design of surface-modified poly(D,L-lactide-co-glycolide) nanoparticles for targeted drug delivery to bone. J Control Release, 122, 24–30.

Dreis S, Rothweiler F, Michaelis M, Cinatl J Jr, Kreuter J, Langer K. (2007). Preparation, characterisation and maintenance of drug efficacy of doxorubicin-loaded human serum albumin (HSA) nanoparticles. Int J Pharm, 341, 207–214.

Finsy R, De Jaeger N. (1991). Particle sizing by photon correlation spectroscopy. Part II: average values. Part Part Syst Char, 8, 187–193.

Garbuzenko O, Barenholz Y, Priev A. (2005). Effect of grafted PEG on liposome size and on compressibility and packing of lipid bilayer. Chem Phys Lipids, 135, 117–129.

Gittens SA, Bagnall K, Matyas JR, Löbenberg R, Uludag H. (2004). Imparting bone mineral affinity to osteogenic proteins through heparin-bisphosphonate conjugates. J Control Release, 98, 255–268.

Godbey WT, Wu KK, Mikos AG. (2001). Poly(ethylenimine)-mediated gene delivery affects endothelial cell function and viability. Biomaterials, 22, 471–480.

Harris JM, Chess RB. (2003). Effect of pegylation on pharmaceuticals. Nat Rev Drug Discov, 2, 214–221.

Hengst V, Oussoren C, Kissel T, Storm G. (2007). Bone targeting potential of bisphosphonate-targeted liposomes. Preparation, characterization and hydroxyapatite binding in vitro. Int J Pharm, 331, 224–227.

Lin R, Liu N, Yang Y, Li B, Liao J, Jin J. (2009). Radioiodination of protein using 2,3,5,6-tetrafluorophenyl 3-(nido-carboranyl) propionate (TCP) as a potential bi-functional linker: synthesis and biodistribution in mice. Appl Radiat Isot, 67, 83–87.

Lin W, Coombes AG, Garnett MC, et al. (1994). Preparation of sterically stabilized human serum albumin nanospheres using a novel Dextranox-MPEG crosslinking agent. Pharm Res, 11, 1588–1592.
Lin W, Garnett MC, Davies MC, et al. (1997). Preparation of surface-modified albumin nanospheres. Biomaterials, 18, 559–565.
Lin W, Garnett MC, Schacht E, Davis SS, Illum L. (1999). Preparation and *in vitro* characterization of HSA-mPEG nanoparticles. Int J Pharm, 189, 161–170.
Merodio M, Arnedo A, Renedo MJ, Irache JM. (2001). Ganciclovir-loaded albumin nanoparticles: characterization and *in vitro* release properties. Eur J Pharm Sci, 12, 251–259.
Meszaros R, Thompson L, Bos M, de Groot P. (2002). Adsorption and electrokinetic properties of polyethylenimine on silica surfaces. Langmuir, 18, 6164–6169.
Mishra V, Mahor S, Rawat A, et al. (2006). Targeted brain delivery of AZT via transferrin anchored pegylated albumin nanoparticles. J Drug Target, 14, 45–53.
Moghimi SM, Hunter AC, Murray JC. (2001). Long-circulating and target-specific nanoparticles: theory to practice. Pharmacol Rev, 53, 283–318.
Nickel J, Dreyer MK, Kirsch T, Sebald W. (2001). The crystal structure of the BMP-2:BMPR-IA complex and the generation of BMP-2 antagonists. J Bone Joint Surg Am, 83-A(Suppl 1), S7–14.
Ogris M, Brunner S, Schüller S, Kircheis R, Wagner E. (1999). PEGylated DNA/transferrin-PEI complexes: reduced interaction with blood components, extended circulation in blood and potential for systemic gene delivery. Gene Ther, 6, 595–605.
Owens DE III, Peppas NA. (2006). Opsonization, biodistribution, and pharmacokinetics of polymeric nanoparticles. Int J Pharm, 307, 93–102.
Perrine TD, Landis WR. (1967). Analysis of polyethylenimine by spectrophotometry of its copper chelate. J Polym Sci A1, 5, 1993–2003.
Pignatello R, Cenni E, Micieli D, et al. (2009). A novel biomaterial for osteotropic drug nanocarriers: synthesis and biocompatibility evaluation of a PLGA-ALE conjugate. Nanomedicine (Lond), 4, 161–175.
Radeva T, Petkanchin II. (1997). Electric properties and conformation of polyethylenimine at the hematite-aqueous solution interface. J Colloid Interface Sci, 196, 87–91.
Schäfer V, von Briesen H, Andreesen R, et al. (1992). Phagocytosis of nanoparticles by human immunodeficiency virus (HIV)-infected macrophages: a possibility for antiviral drug targeting. Pharm Res, 9, 541–546.
Segura S, Espuelas S, Renedo MJ, Irache JM. (2005). Potential of albumin nanoparticles as carriers for interferon gamma. Drug Dev Ind Pharm, 31, 271–280.
Soppimath KS, Aminabhavi TM, Kulkarni AR, Rudzinski WE. (2001). Biodegradable polymeric nanoparticles as drug delivery devices. J Control Release, 70, 1–20.
Sung SJ, Min SH, Cho KY, et al. (2003). Effect of polyethylene glycol on gene delivery of polyethylenimine. Biol Pharm Bull, 26, 492–500.
Tang GP, Zeng JM, Gao SJ, et al. (2003). Polyethylene glycol modified polyethylenimine for improved CNS gene transfer: effects of PEGylation extent. Biomaterials, 24, 2351–2362.
Tye CE, Rattray KR, Warner KJ, et al. (2003). Delineation of the hydroxyapatite-nucleating domains of bone sialoprotein. J Biol Chem, 278, 7949–7955.
Uludag H. (2002). Bisphosphonates as a foundation of drug delivery to bone. Curr Pharm Des, 8, 1929–1944.
Uludag H, Yang J. (2002). Targeting systemically administered proteins to bone by bisphosphonate conjugation. Biotechnol Prog, 18, 604–611.
Vail NK. (2005). Skeletally targeted nanoparticles. WO/2005/020965.
Vail NK. (2008). Targeted delivery of bioactive factors to the systemic skeleton. US 7 381 426 B2.
Varkey M, Kucharski C, Haque T, Sebald W, Uludag H. (2006). *In vitro* osteogenic response of rat bone marrow cells to bFGF and BMP-2 treatments. Clin Orthop Relat Res, 443, 113–123.
von Harpe A, Petersen H, Li Y, Kissel T. (2000). Characterization of commercially available and synthesized polyethylenimines for gene delivery. J Control Release, 69, 309–322.
Wang D, Miller S, Sima M, Kopecková P, Kopecek J. (2003). Synthesis and evaluation of water-soluble polymeric bone-targeted drug delivery systems. Bioconjug Chem, 14, 853–859.
Wang D, Miller SC, Kopecková P, Kopecek J. (2005). Bone-targeting macromolecular therapeutics. Adv Drug Deliv Rev, 57, 1049–1076.
Wang G, Siggers K, Zhang S, et al. (2008). Preparation of BMP-2 containing bovine serum albumin (BSA) nanoparticles stabilized by polymer coating. Pharm Res, 25, 2896–2909.
Zhang S, Wright JE, Ozber N, Uludag H. (2007). The interaction of cationic polymers and their bisphosphonate derivatives with hydroxyapatite. Macromol Biosci, 7, 656–670.
Zhang S, Wang G, Lin X, et al. (2008). Polyethylenimine-coated albumin nanoparticles for BMP-2 delivery. Biotechnol Prog, 24, 945–956.
Zhang S, Doschak MR, Uludag H. (2009). Pharmacokinetics and bone formation by BMP-2 entrapped in polyethylenimine-coated albumin nanoparticles. Biomaterials, 30, 5143–5155.
Zhang S, Kucharski C, Doschak MR, Sebald W, Uludag H. (2010). Polyethylenimine-PEG coated albumin nanoparticles for BMP-2 delivery. Biomaterials, 31, 952-963.